Hydrodynamics of binary mixture fluidization in a compartmented fluidized bed

A.V. Gorin, V.S. Chok, S.K. Wee, H.B. Chua, [1]H.M. Yan
Curtin Univ. of Technology, Sarawak Campus, CDT 250, 98009 Miri, Sarawak, Malaysia; e-mail: alexander.g@curtin.edu.my. [1]The University of Queensland, St Lucia, 4072, QLD, Australia; e-mail: h.yan@uq.edu.au

Abstract - The paper represents an extensive study of hydrodynamic characteristics of a fluidized bed in a pilot-plant-scale fluidized bed reactor designed for syngas production and power generation from biomass as a source of renewable energy. An air-blown compartmented fluidized bed gasifier permitting heat transfer between adjacent discrete compartments via solid circulation consists of two compartments, the combustor and the gasifier, operating at bubbling fluidized mode.

Results of numerical simulation of the fluidized bed containing monodispersed size Geldart B particles are represented. A three-dimensional Eulerian-eulerian granular model with closure laws according to the kinetic theory of granular flow is chosen to simulate the multiphase environs at 0.2 – 3.2 times minimum fluidization velocity.

The present work reports also experimental results on the fluidization of palm shell-sand binary mixtures of 2, 5, 10, and 15 wt% of feedstock including the minimum fluidization velocity of palm shell-sand binary mixtures, fluidization quality for different bed diameter, particle size, bed height, and superficial velocity. The vertical and lateral palm shells distributions in the mixtures are also discussed.
***Keywords*:** Binary mixtures, fluidization, CFD, biomass

1. INTRODUCTION

Fluidized bed is selected for gasification process due to its effectiveness of heat and mass transfer between the gas and solid phases [1]. Although this process is considered as one of the oldest technologies and has been made successful in some industrial-scale production of renewable energy from biomass, generally this industry still faces a lot of challenges including the availability of economically viable technology, sophisticated and sustainable natural resources management, and proper market strategies under competitive energy markets [2].

Most of the present gasifiers are oxygen-blown to maintain its calorific value and to prevent nitrogen contamination in the product gas. Oxygen is obtained from air separation unit, which imposes heavy capital and operation unit, which impose heavy capital and operating costs to any conventional gasification plant.

Compartmented Fluidized Bed Gasifier (CFBG) (for an extensive list of references see [3]) is capable of producing high calorific value syngas (>11 MJ/Nm^3) with full compatibility for existing power generation and chemical synthesis technologies, without the needs of pure oxygen. CFBD permits heat transfer between adjacent discrete compartments via solid circulation consists of two compartments, the combustor and the gasifier, operating at bubbling fluidized mode.

Wu et al. [4] has reviewed the various minimum fluidization velocity, U_{mf}, correlations for multicomponents system. These correlations were based on two distinct features, either requiring the determination of single component U_{mf} or as a whole. The latter is more likely applicable to biomass as the components cannot be solely fluidized [5]. Rao et al. [5] developed correlation from a 5cm ID reactor using rice husks, sawdust and groundnut shell powder, up to 15 wt% with sands. Noda et al. [6] developed correlation using glass beads, wood, marten shot, soybean, small bean, and rubber with sands in 16cm ID column. It is found that the U_{mf} strongly depends on the mixing condition in the bed and on the volume fraction of the fluidizing medium. The authors have developed correlation with standard deviation of ±35%. All the above-mentioned correlations have not been tested using the present biomass/sand mixtures and in large reactor where the mixing state is very much scale-dependent.

Vertical and lateral mixing of palm shells in mixture is of great importance to the reactor performance as well. In fluidized bed, mixing mechanism is governed by bubble bursting and displacement, which provoke particles vertical and horizontal motion. A gas fluidized bed containing a mixture of particles of differing densities will segregate into two layers if the density ratio differs significantly from unity [7]. Some previous studies and reviews have been conducted to investigate mixing/segregating behavior in binary mixtures [4, 8-11]. Papers [4, 9] report data on equidensity binary systems; mixing characteristic of different particle densities and sizes (≤ 928μm) are represented in [10]. Shen et al. [11] studied binary system but limited to 2-D bed.

Despite of the fact that CFD is at the development stage for multiphase systems such as fluidized beds, numerical simulation allows getting round many problems related to complex and expensive experiment in fluidized bed. The Eulerian-eulerian model treating each phase as continuous and interpenetrating continuum is the preferred choice for simulating macroscopic hydrodynamic parameters due to relative simplicity and reasonable computational time. The bubbles motion and properties has been examined in 2D and 3D simulations [12, 13]. Paola et al, [14], reported that the 2D and 3D simulations show similar voidage profile and consistent formation, shape and size of bubbles for uniform shape of reactor. A few authors, [12-17], carried out the modeling using Geldart A and Geldart B particles incorporated with different drag laws.

In this study, the Eulerian-eulerian CFD model has been applied to study the hydrodynamics of CFBG in terms of the pressure drop, bed expansion and voidage profiles at the gasifier side. The simulated results are then compared with experimental results for model validation.

The objectives of this study are, first, to apply the Eulerian-eulerian CFD model for study of the hydrodynamics of CFBG in terms of the pressure drop, bed expansion and voidage profiles at the gasifier side, and secondly, to provide data and practical recommendations for pilot-scale CFBG from experimental investigation of binary mixture hydrodynamics.

Palm shell is selected as gasification feedstock in view of its great potential in feasibility of syngas production and due to its abundance supply since oil palm is ranked as number 1 fruit crops produced in year 2007 [2].

The experiments are carried out on fluidization of palm shell-sand binary mixtures of 2, 5, 10, and 15 wt% of palm shells in CFBG cold model of 66cm ID consisting of 2 compartments, combustor and gasifier with 2:1 ratio respectively, fluidized with air. The U_{mf} of these mixtures of different wt% is determined and compared with published U_{mf} correlations developed for small diameter column and different biomasses. Fluidization quality, Q, at different bed diameter, D, bed height, H, superficial velocity, U_o, and palm shell sizes and wt% are studied. The vertical and lateral palm shells distributions in these mixtures are also presented.

2. COMPUTATIONAL MODEL

The simulation of 3-D fluidized bed in the complex geometry CFBG is performed by using the CFD commercial package, FLUENT 6.3.26. A multi-fluid Eulerian-eulerian model, which considers the conservation of mass and momentum for the gas and fluid phases, supplemented by kinetic theory of granular flow to describe the solid phase stress can be summarized as below:

Mass conservation equations of gas (g) and solid (s) phases:

$$\frac{\partial}{\partial t}.(\alpha_g.\rho_g) + \nabla.(\alpha_g.\rho_g.\vec{v}_g) = 0 \quad (1)$$

$$\frac{\partial}{\partial t}.(\alpha_s.\rho_s) + \nabla.(\alpha_s.\rho_s.\vec{v}_s) = 0 \quad (2)$$

Momentum conservation equations of gas and solid phases:

$$\frac{\partial}{\partial t}.(\alpha_g.\rho_g.\vec{v}_g) + \nabla.(\alpha_g.\rho_g.\vec{v}_g^{\,2}) = -\alpha_g.\nabla p + \nabla.\bar{\bar{\tau}}_g + \alpha_g.\rho_g.\vec{g} + K_{gs}.(\vec{v}_g - \vec{v}_s) \quad (3)$$

$$\frac{\partial}{\partial t}.(\alpha_s.\rho_s.\vec{v}_s) + \nabla.(\alpha_s.\rho_s.\vec{v}_s^{\,2}) = -\alpha_s.\nabla p - \nabla p_s + \nabla.\bar{\bar{\tau}}_s + \alpha_s.\rho_s.\vec{g} + K_{gs}.(\vec{v}_g - \vec{v}_s) \quad (4)$$

Fluctuation energy conservation of solid particles

$$\frac{3}{2}.\left[\frac{\partial}{\partial t}.(\rho_s.\alpha_s.\Theta_s) + \nabla.(\rho_s.\alpha_s.\vec{v}_s.\Theta_s)\right] = (-p_s\bar{\bar{I}} + \bar{\bar{\tau}}_s) : \nabla.\vec{v}_s + \nabla.(k_{\Theta s}.\nabla.\Theta_s) - \gamma_{\Theta s} \quad (5)$$

Table 1: Momentum exchange coefficients

Gidaspow drag function

$$K_{gs} = \frac{3}{4}.C_D.\frac{\alpha_s.\alpha_g.\rho_g.\left|\vec{v}_s - \vec{v}_g\right|}{d_s}.\alpha_g^{-2.65} \qquad \text{for } \alpha_g > 0.8$$

$$K_{gs} = 150.\frac{\alpha_s^2.\mu_g}{\alpha_g.d_s} + 1.75.\frac{\alpha_s.\rho_g.\left|\vec{v}_s - \vec{v}_g\right|}{d_s} \qquad \text{for } \alpha_g \le 0.8$$

$$C_D = \frac{24}{\alpha_g.\mathrm{Re}_s}.[1 + 0.15.(\alpha_g.\mathrm{Re}_s)^{0.687}] \qquad \text{and}$$

$$\mathrm{Re}_s = \frac{\rho_g.d_s.\left|\vec{v}_s - \vec{v}_g\right|}{\mu_g}$$

The constitutive equations as recommended in FLUENT user guide [18] are needed to close the governing relations. The momentum exchange coefficient can be calculated by specifying drag functions as shown in Table 1. Despite of rigorous mathematical modeling the drag laws used in the model continue to be semi-empirical in nature. Therefore, it is crucial to use a drag law that correctly predicts the incipient fluidization conditions. In this study, Gidaspow drag function is applied as it is proposed for modeling dense fluidized beds [18, 19].

The governing equations are solved by finite volume method. First-order discretization schemes for the convection terms are used. A time step of 0.001s with 10 iterations per time step is chosen. This iteration is adequate to achieve convergence.

Table 2: Simulation model parameters

Description	Value	Unit
Height of reactor	1.50	m
Particle density, ρ_p	2620	kg/m^3
Air density, ρ_g	1.2	kg/m^3
Mean particle diameter, d_p	272	μm
Restitution coefficient	0.9	-
Initial volume fraction	0.45	-
Superficial velocity, U	0.02 - 0.2	m/s
Static bed height	0.3	m
Grid interval spacing	0.2	cm
Inlet boundary conditions	Velocity	-
Outlet boundary conditions	Pressure	-
Time steps	0.001	s
Maximum number of iterations	10	-
Convergence criteria	10^{-3}	-

The relative error between two successive iterations is specified by using a convergence criterion of 10^{-3} for each scaled residual component. The phase-coupled SIMPLE algorithm is applied for the pressure-velocity coupling. Table 2 gives a summary of the flow parameters to be used in the simulation of 3D fluidized bed (gasifier).

3. EXPERIMENTAL SETUP AND METHODOLOGY

A pilot-scale compartmented fluidized bed gasifier (Fig.1) of the overall diameter of 0.66m with a height of 1.8m,

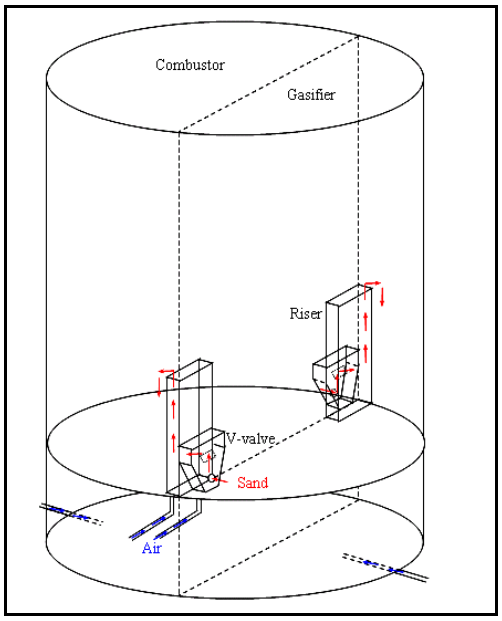

Fig. 1. Isometric view of CFBG

partitioned into two compartments, the combustor and the gasifier, in a ratio of 65:35 respectively.

Perforated plate distributor is used to uniformly distribute the fluidizing agent, ambient air at free area of 0.27% and 0.32% for the gasifier and combustor accordingly. The air flow rate is regulated relative to the minimum fluidization velocity, U_{mf}, between 1-2.5U_{mf} by rotameters (Fig. 2) to maintain the bubbling mode of fluidization. Pressure drops, ΔP, are measured using water manometers at 3 different positions to indicate the total ΔP, across the distributor and bed respectively. The inert particles used are the Geldart B particles, river sand, of 272 μm in mean size diameter and 2620 kg/m^3 in density. Palm shell with moisture less than 10wt% and density of 1200kg/m^3 consists of 3 mean diameter (d_{ps}) of 1.77, 3.55 and 13.95mm (with respective size ranges of 1.18-2.36, 2.36-4.75 and 4.75-9.20mm). The present work studies the fluidization of biomass-sand binary mixtures of 0 (no feedstock), 2, 5, 10, and 15 wt%. Design of the experimental set-up allows visual observation during the experiment.

The standard experimental approach in determining monodisperse U_{mf}, is based on defluidization stage of ΔP-U_o profile. U_{mf} is estimated from the intersection point of the fixed bed line with the constant pressure line. Though the profile and consequently, the determination of binary U_{mf} would generally be affected by different initial conditions [9], the defluidization stage where the components are already mixed is preferred because they are more representative of binary system existing as a "single" bed material.

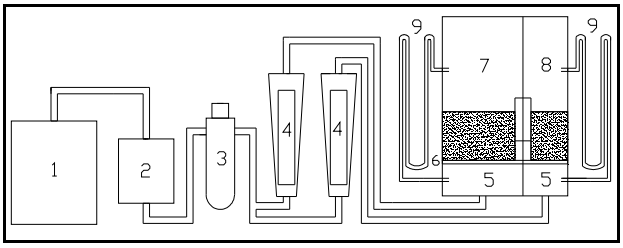

Fig. 2. Experimental set up (1: compressor; 2: dryer; 3: pressure regulator; 4: rotameter; 5: plenum; 6: perforated plate distributor; 7: combustor; 8: gasifier; 9: manometers).

For the fluidization quality, Q, defined as experimental bed pressure drop / static weight per unit area, the bed ΔP is computed by subtracting distributor ΔP from total ΔP.

"Thief" probe (diameter 5cm) and sieving method are preferred due to fast response and the ability of collecting samples while the bed is fluidized at different locations in the bed under various operating conditions.

The probe is removed vertically from the bed. The mixtures is then sieved and weighed to determine their component weight fraction.

Prior to the experiments, sands are filled to desired weight/height and packed. Palm shells are then uniformly stacked on the bed surface forming two segregated layers. This approach is selected to track palm shell migration. The U_{mf}, Q, and solids mixing behavior are simultaneously measured. Solid sample is collected from 3 different sections (v-valve, center and riser) in 3 different levels (L1 to L3 indicating top, center, bottom), which constitutes 9 imaginary cells (n) shown in Fig. 3.

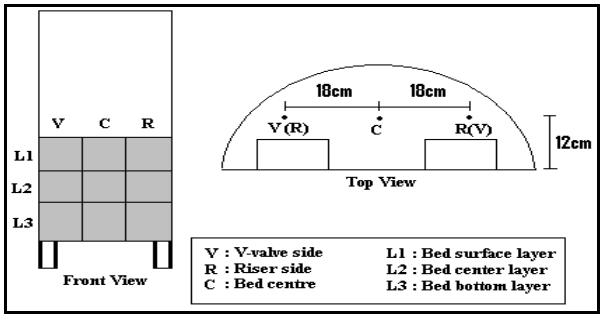

Fig. 3. Sampling locations in gasifier (those in brackets represent combustor side)

Data on mixing is presented graphically such that the deviation of the perfect mixing line indicates segregation. Vertical or lateral mixing index, m, is defined as local palm shell wt% / load palm shell wt% or (x/X). m=1 represent perfect mixing, while segregation may lead to two conditions, either "dilution" (m<1) or accumulation (m>1). Assuming that 9 locations are able to represent the whole bed composition, the overall mixing index, M, can therefore

be computed, in absolute terms according to the equation

$$M = 1 - \left(\frac{1}{n}\right)\left(\frac{|local\ PS\ wt\% - load\ PS\ wt\%|}{load\ PS\ wt\%}\right) \qquad (6)$$

Values m=1 and m <1 correspond to perfect mixing and segregation respectively. Three repetitive data are taken in each location with standard deviation of ±15%. Each set is in 15 minutes interval to allow steady state. Shen L.H et al. [11] observed that equilibrium mixing is achieved in 10 seconds. Notwithstanding of the measurement for the study of the effect of bed height to Q and mixing, all the experiments are conducted at constant total bed weight of 77kg.

4. RESULTS AND DISCUSSION

COMPARISON OF NUMERICAL SIMULATION WITH EXPERIMENTAL RESULTS

The CFD simulations are carried out under transient state condition. Various superficial gas velocities from 0.02 to 0.2 m/s, which correspond to 0.3 – 3.2$U_{mf,}$ are examined.

A comparison of the time-averaged bed pressure drop against superficial gas velocity is plotted in Fig.4. At U < $U_{mf,}$ the simulation results overestimate the bed pressure drop. The results show better agreement at velocities greater than U_{mf}. This discrepancy at lower velocities may be attributed to the dominant interparticle frictional forces, which are not predicted by the multi-fluid model for simulating gas-solid phases [20]. Moreover, the drag model employed does not take into account effect of complex geometry at the gasifier side. The standard deviation of ±10% is observed for the simulation results in comparison with experimental results.

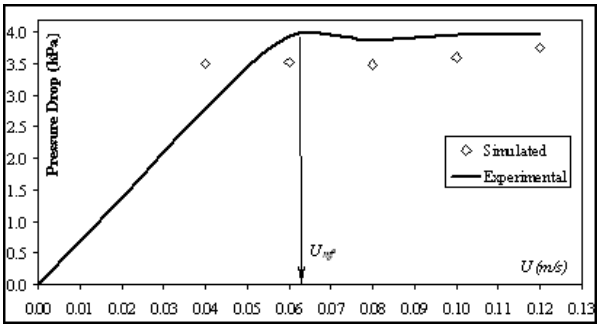

Fig. 4. Comparison of experimental and simulated bed pressure drop (e_{ss} = 0.9, H_o = 0.3m)

Figure 5 illustrates the comparison of experimental and simulated bed expansion ratio. The simulation results demonstrate the consistent increase in bed expansion with gas velocity and predict the bed expansion reasonably well (max ± 6%) for Geldart B particles. The over-prediction of bed expansion as discussed in other studies [19, 20] does not occur in our study; it is discernible that the model pertinently estimated the bed fluidization behavior in this work.

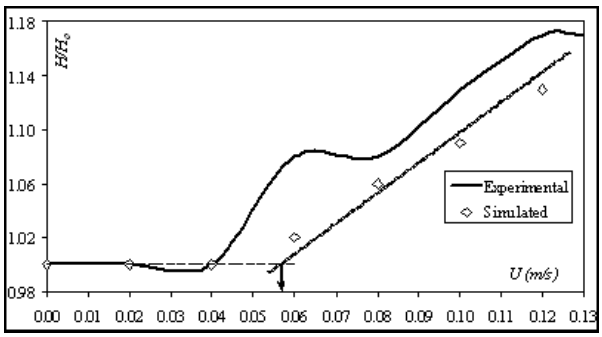

Fig. 5. Comparison of experimental and simulated bed expansion ratio (e_{ss} = 0.9, H_o = 0.3m)

As can be observed in Fig. 4, the U_{mf} cannot be determined from the simulated results using typical pressure drop vs velocity profile. However, it can be obtained from the interception point of the constant expansion ratio line at U < U_{mf} during static state with the gradual increased expansion ratio line for U > U_{mf} where the bed expands in Fig. 5. The numerically obtained U_{mf} is 0.057 m/s as compared to the experimentally determined U_{mf} = 0.062m/s.

Fig. 6 shows a contour plot of solids fraction viewing at the central part of gasifier front wall. At time 0.0s, the bed remains static. At early stage, waves of voidage are created (probably analogous to the continuity waves [21]), which travel through the bed and subsequently break to form bubbles as the process progresses. The bed height increases with bubble formation until it levels off at a steady-state bed height. The chaotic transient generation of bubble formation can be seen after 2.0s.

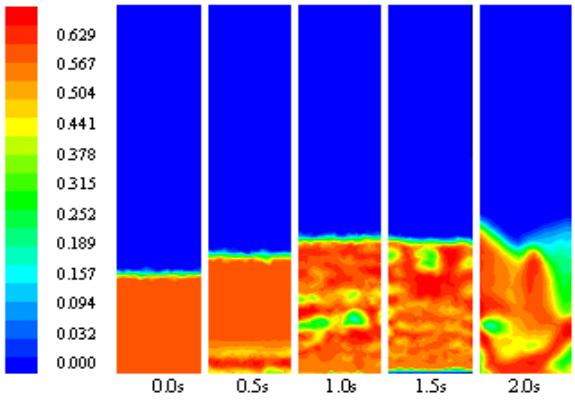

Fig. 6: Simulated solids volume fraction profile (front view, U = 0.2m/s)

The fluidization quality, Q, is defined as the ratio of experimental bed pressure drop to the static weight per cross sectional area of the bed. As can be seen from Fig. 7, no distinctive differences are observed with increase in bed height. The average quality over the range is approximately 0.8. The behavior of the fluidization is, in fact, an indication of channeling bed, where there is localized de-fluidization that leads to not fully suspended bed at gasifier. More

studies have been carried out on the quality aspect elsewhere [22, 23].

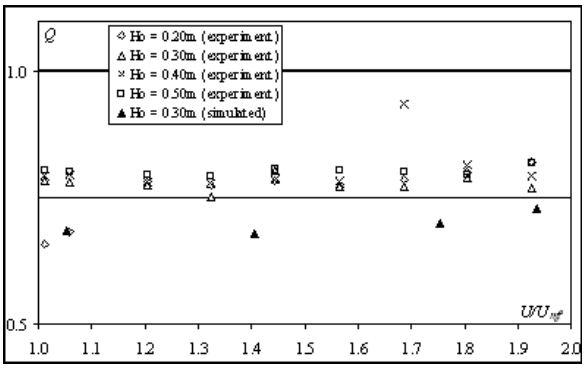

Fig. 7. Fluidization quality, Q, versus U/U_{mf} at different bed height

EXPERIMENTAL DATA ON BINARY MIXTURE

Generally, an increase in palm shell size or wt% leads to an increase in U_{mf}. From Table 3, it is obvious that Noda's et al. [6] correlation developed from combination of the component U_{mf} is not applicable to the mixtures where the biomass can not be solely fluidized, similarly to that high - lighted by Bilbao et al. [24] in sand/straw binary mixtures. Rao et al. [5] prediction is relative closer but significantly underestimates due to different bed characteristics, e.g. the sphericity and bed incipient porosity (ϕ=0.86, ε_{mf}=0.42) differ from those for the present system (ϕ=0.54, ε_{mf}=0.34).

Table 3. Experimental (Exp) data, correlations results and percentage error (ER%) for various palm shell size and wt%.

Palm Shell wt%; d_{ps}(mm)	U_{mf} (m/s)				
	Exp	Noda et al [6]	ER %	Rao et al [5]	ER %
2%; 3.55	0.045	0.555	1110	0.025	-44
5%; 3.55	0.045	0.553	1130	0.031	-31
10%; 1.77	0.055	0.490	791	0.038	-31
10%; 3.55	0.055	0.568	930	0.044	-20
10%; 13.95	0.067	0.671	901	0.060	-10
15%; 3.55	0.076	0.583	670	0.066	-13

Fluidization Quality

Experiments show, the increase in the bed diameter and palm shell sizes provides no significant changes in the Q value for the binary components. There were no also distinctive changes in the Q value with different bed aspect ratio, H/D (constant D, increasing H). A through-channeling is observed, and fluctuation becomes more intense with the increase in palm shell wt% (a single component bed has higher Q value than binary component in gasifier, and in single component experiments, the through-channeling changes to intermediate-channeling as the particle diameter increases). In Fig. 8 (from here on, experimental data for the palm shell size d_{ps} = 3.53 mm are presented), $Q \approx 0.8$ in single component while Q fluctuates between 0.6-0.7 in binary mixtures. This is due to the differing shape, size and density of the binary components, leading to more severe local pressure/density variation. Rhodes [25] stated that bubbles formed in group B and D particles will continue to grow but never achieve a maximum size associated with large pressure fluctuations.

Palm shell used in this study and classified as Geldart D [26] has a tendency to produce spouted beds. The effective particle size and bed voidage will increase while the effective density decreases, when the palm shell wt% increases in the mixtures. Abdullah et al. [27] stated that bulk density and voidage are the two main factors contributing to the bed fluidization quality.

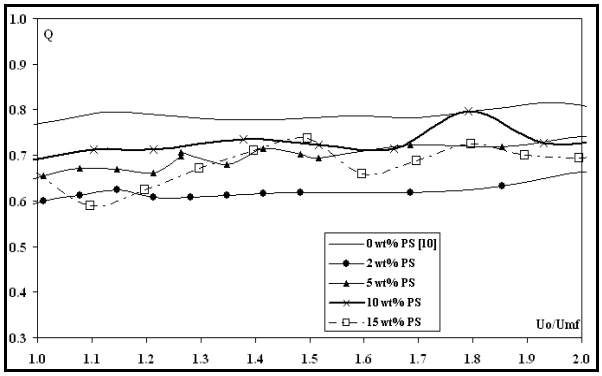

Fig. 8. Q versus U_o/U_{mf} at different palm shell wt%

Vertical and lateral mixing

Figure 9 shows the typical palm shell vertical distribution at various U_{mf} for 10 wt%-load of palm shell. Vertical mixing enhances with the U_{mf} increase approaching maximum accumulated value is M=10, if a collected sample is purely palm shell. However, palm shells with lower density, tends to migrate towards the bed surface due to easiness of being swept away by the air through flow from distributor and carried up by rising bubbles. At higher U_o, (2.0-2.5U_{mf}), palm shells tend to become uniformly mixed, resulting in a smaller palm shells concentration gradient developed along the bed height.

Typical palm shell lateral distribution with various U_{mf} is shown in Fig. 10. Overall, the M indexes of three layers improve with increasing U_o.

Lateral mixing of solids in a gas solid fluidized bed is caused by two mechanisms, which are bursting bubbles at the bed surface and bubbles displacement inside the bed [26]. At 1.25U_{mf} lateral mixing is initiated by bursting bubbles at the bed surface where a large fraction of the palm shells at the centre is dispersed. At L2 and L3, the mixing induced by bubbles displacement is insignificant. With increasing U_o (from 1.5 to 2.5U_{mf}), lateral palm shells distributions across fluidized bed at L1, L2, and L3 approach each other due to increasing bubbling rate, whereby lateral mixing induced by bubbles displacement

becomes more significant resulting in enhanced lateral mixing.

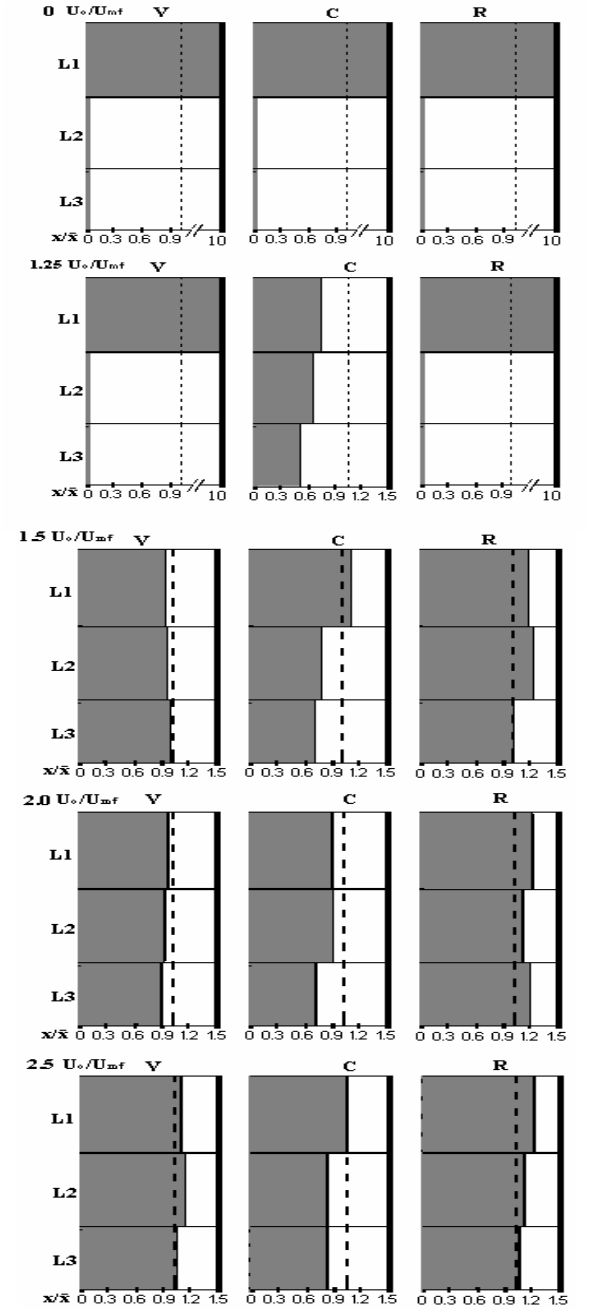

Fig. 9. Effect of U_o/U_{mf} on vertical mixing for 10 wt%

Generally, the increase of superficial velocity U_o will improve mixing in segregated systems of mixtures with different densities/sizes [28]. Shen et al. [29] reported that the wake exchange coefficient, which indicates vertical and lateral solid mixing intensity, reduced with the increase in U_{mf}. On the contrary, in Fig. 11, *M*-index increases although U_{mf} increases with palm shell wt%. This is likely due to the increase in ε_{mf} (Table 4) that leads to greater bed expansion, allowing effective vertical and lateral solid mixing.

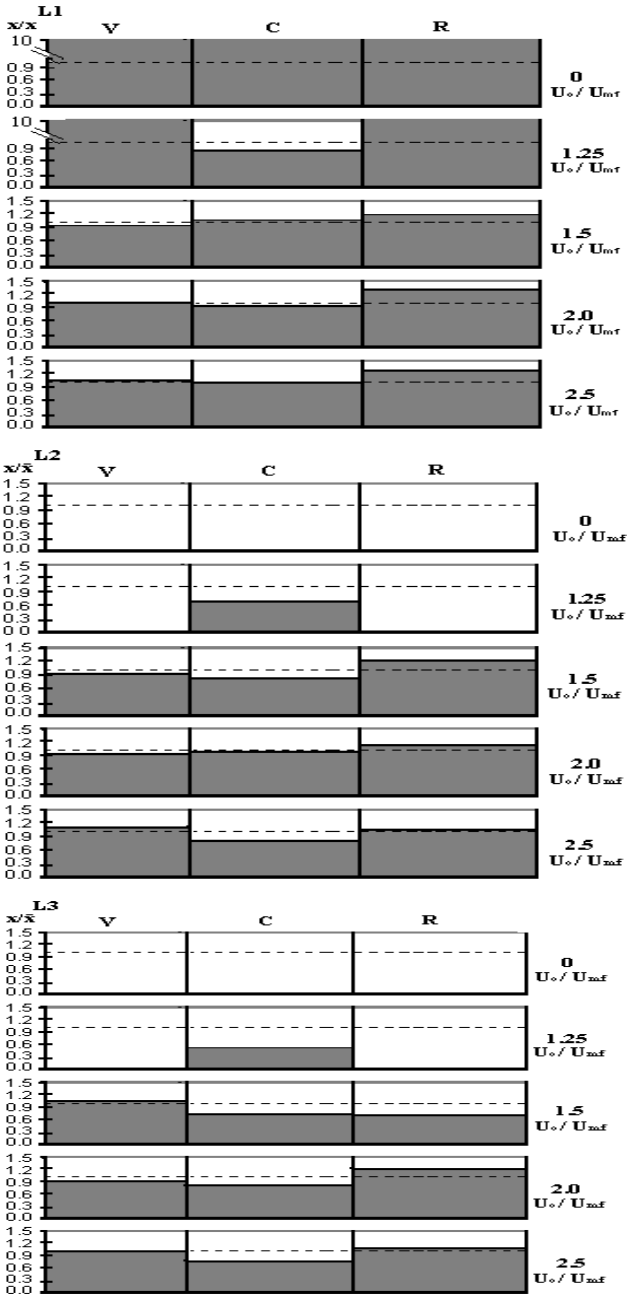

Fig. 10. Effect of U_o/U_{mf} on lateral mixing for 10 wt%

In Fig. 12, maximum overall mixing index is achieved at $1.5U_{mf}$ for deep bed, whereas at shallow bed, the same degree of mixing is only achievable at higher U_o ($\geq 2U_{mf}$).

With increasing bed height, the bed pressure drop increases resulting in a stable bubbling across bed distributor and uniform mixing of the fluidized bed. Conversely, in shallow beds, where the total bed pressure drop is reduced, the local preferential channeling forms. This contributes to non-uniform bubbling at the expense of the rest of the bed [30]. Therefore, if U_o is held constant, poorer mixing occurs with a sensitivity to bed height in shallow beds and relatively good mixing in deep beds.

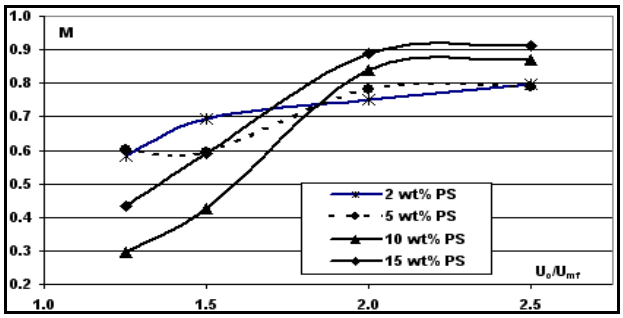

Fig. 11. Effect of palm shell wt% on overall mixing index

Table 4: Bed voidage at U_{mf} for various palm shell wt%.

Palm Shell wt%	2	5	10	15
ε_{mf}	0.32	0.33	0.36	0.37

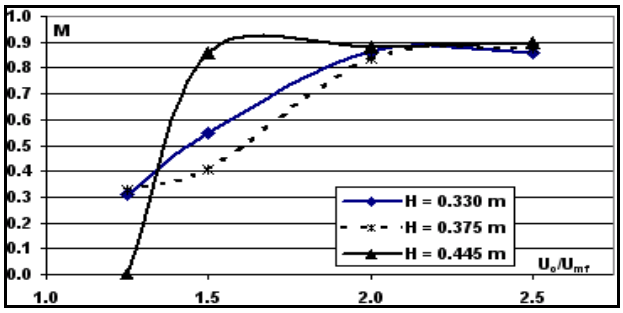

Fig. 12. Effect of bed height on overall mixing index of 10 wt% palm shell

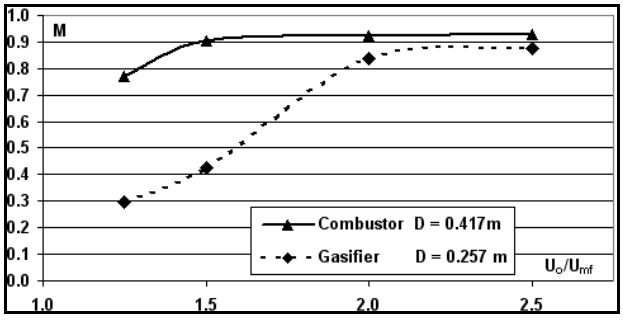

Fig. 13. Effect of bed diameter on overall mixing index of 10 wt% palm shell

In Fig. 13, the combustor of a larger bed diameter attained the higher overall mixing index at lower U_o ($1.5U_{mf}$). The flow behavior of a gas solid fluidized bed is highly sensitive to the scale [30]. In the gasifier of smaller bed diameter, the presence of v-valve and riser, contributes to greater wall effect as compared to the combustor, resulting significant reduction in the overall growth of bubbles [31]. As the diameter increases, the wall effect becomes insignificant, hence enhancing vertical mixing. The lateral mixing is also enhanced with increasing bed width [27]. These combined effects improve the overall mixing index.

5. CONCLUSION

Numerical simulation shows reasonably well agreement with experimental results in terms of bed pressure drop, bed expansion ratio and minimum fluidization velocity.

From experimental study of CFBG hydrodynamics it follows that the minimum fluidization velocity correlations developed from small-scale laboratory reactors and different biomasses could not be extended to the present system. No significant effect on the fluidization quality value with respect of different geometry, particle sizes, bed height, and wt% of palm shells and through-channeling is observed throughout the experiments. However, it is found that the single component demonstrates the higher fluidization quality values compared with those for binary mixtures. It is interesting to note that uniform mixing is attainable for binary system studied even though the fluidization quality value less than 0.8.

As for mixing/segregation, the mixing indexes m and M increase with the superficial velocity increase. The bed diameter has more dominant effect as compared to the wt% and size of the feedstock; larger bed diameter and bed high require lower superficial velocity to achieve good mixing. There is an optimum value of the velocity where uniform mixing ($M \geq 0.85$) can be established, and it is found to be 1.5-2 times the minimum fluidization velocity over the whole range of experimental parameters studied.

6. NOMENCLATURE

C_D	drag coefficient
D	bed diameter
d	diameter, m
e_{ss}	restitution coefficient
g	gravitational force, m/s^2
H	expanded bed height, m
H_o	static bed height, m
$\overline{\overline{I}}$	stress tensor
$k_{\Theta s}$	diffusion coefficient for granular energy, kg/sm
K_{gs}	gas/solid momentum exchange coefficient
m	vertical or lateral mixing index
M	overall mixing index
Q	fluidization quality
Re	Reynolds number
t	time, s
U_0	superficial gas velocity, m/s
v	velocity, m/s

Greek letters

α	volume fraction
γ_Θ	collision dissipation energy, kg/s^{3}m
ε	voidage
Θ	granular temperature, m^2/s^2
μ	shear viscosity, kg/sm
ρ	density, kg/m^3
$\overline{\overline{\tau}}$	stress tensor, Pa

Subscripts

g	gas
mf	minimum fluidization
s	solids

REFERENCES

[1] W. Ragnar, "Gasification of biomass: comparison of fixed bed and fluidized bed gasifier," *Biomass and Bioenergy*, vol. 18, 2000, pp. 489 – 497.

[2] T.L.K. Yong, K.T. Lee, A.R. Mohamed, S. Bhatia, "Potential of hydrogen from oil palm biomass as a source of renewable energy worldwide," *Energy Policy* vol. 35, 2007, pp. 5692 – 5710.

[3] V.S. Chok, S.K. Wee, A. Gorin, H.B. Chua, H.M. Yan, 2007 Compartmented fluidized bed gasifier for syngas production and power generation from biomass// 12th Int Energy Conference and Exhibition 'Energex 2007', Singapore

[4] S.Y. Wu, J. Baeyans, "Segregation by size difference in gas fluidized beds,", *Powd. Tech.*, vol. 98, 1998, pp. 139- 150.

[5] T.R. Rao, J.V. Ram. Bheemarasetti (2001), "Minimum fluidization velocity of mixtures of biomass and sands," *Energy*, vol. 26, 2001, pp. 633 – 644.

[6] K. Noda, S. Uchida, T. Makino, H. Kamo, "Minimum fluidization velocity of binary mixtures of particles with large size ratio," *Powd. Tech.*, vol. 46, 1986, pp.149–154.

[7] J. M. Beeckmans, B. Stahl, "Mixing and segragation kinetics in a strongly segregated gas-fluidized bed," *Powd. Tech.*, vol. 53(1), 1978, pp. 31 – 38.

[8] Q.Q. Sun, H.L. Lu, W.T. Liu, Y.R. He, L.D. Yang, D. Gidaspow, "Simulation and experiment of segregating/mixing of rice husk-sand mixtures in a bubbling fluidized bed," *Fuel*, vol. 84, 2005, pp. 1739 – 1748.

[9] B. Formisani, G. De Cristofaro, R. Girimonte, "A fundamental approach to the phenomenology of fluidization of size segregating binary mixtures of solids," *Chem. Eng. Sci.*, vol. 56, 2001, pp. 109 – 119.

[10] A.W. Nienow, P.N. Rowe, L.Y.L. Cheung, "A quantitative analysis of the mixing of two segregating powders of different density in a gas-fluidized bed," *Powd. Techn.*, vol. 20, 1978, pp. 89 – 97.

[11] L.H. Shen, J. Xiao, F. Niklasson, F. Johnsson, "Biomass mixing in a fluidized bed biomass gasifier for hydrogen production," *Chem. Eng. Sci.*, vol. 62, 2007, pp. 636 – 646.

[12] P.J. Witt, J.H. Perry, and M.P. Schwarz, "A numerical model for predicting bubble formation in a 3D fluidized bed", *Appl. Math. Modelling*, vol. 22, 1998, pp. 1071 – 1080.

[13] Ian Hulme, Eric Clavelle, Loni can der Lee, and Apostolos Kantzas, "CFD modelling and validation of bubble properties for a bubbling fluidized bed", *Ind. Eng. Chem*., 2005, vol. 44, pp. 4254 – 4266.

[14] Paola L., Giorgio M., Luca C., and Derek C., "Computational Fluid Dynamics simulations of gas fluidized beds: a preliminary investigation of different modelling approaches", *Proc. 10th Workshop on Two-phase Flow Predictions*, Meseburg, 2002, pp. 300-309.

[15] R. Krishna and J.M. van Baten, "Using CFD for scaling up gas-solid bubbling fluidised bed reactors with Geldart A powders", *Chem. Eng. Jl*, 2001, vol. 82, pp. 247 – 257.

[16] Tim Mckeen and Todd Pugsley, "Simulation and experimental validation of a freely bubbling bed of FCC catalyst", *Powd. Tech.*, 2003, vol. 129, pp. 139 – 152.

[17] M.J.V. Goldschmidt, J.A.M. Kuipers, and W.P.M. van Swaaij, "Hydrodynamic modelling of dense gas-fluidised beds using the kinetic theory of granular flow: effect of coefficient of restitution on bed dynamics", *Chem. Eng. Sci.*, 2001, vol. 56, pp. 571 – 578.

[18] FLUENT, 2002. Fluent 6.0 User's Guide, 20.4 Eulerian Model. Fluent Inc.

[19] Sebastian Zimmermann and Fariborz Taghipour, "CFD modelling of the hydrodynamics and reaction kinetics of FCC fluidized-bed reactors", *Ind. Eng. Chem*., 2005, vol. 44, pp. 9818 – 9827.

[20] Fariborz Taghipour, Naoko Ellis, and Clayton Wong, "Experimental and computational study of gas-solid fluidized bed hydrodynamics", *Chem. Eng. Sci.*, 2005, vol. 60, pp. 6857 – 6867.

[21] Graham B. Wallis, "One-dimensional Two-phase Flow", 1969, McGraw-Hill.

[22] Siaw K. Wee, Vui S. Chok, C. Srinivasakannan, Han B. Chua, and Hong M. Yan, "Fluidization quality study in a compartmented fluidized bed gasifier (CFBG)", *Energy & Fuels*, 2007, Vol. 21.

[23] S.K. Wee, V.S. Chok, B. Chin, W.W. Tang, A. Gorin, H.B. Chua, and H.M. Yan, "On the effect of effective diameter on fluidization quality in compartmented fluidized bed gasifier", *Proc. SOMChE*, 2007, Kuala Lumpur, Malaysia, 2007.

[24] R. Bilbao, J. Lezaun, J.C. Abanades, "Fluidization velocities of sand/straw binary mixtures," *Powd. Tech.*, vol. 52, 1987, pp. 1 – 6.

[25] M. Rhodes, *Introduction to particle technology*, John Wiley & Sons, England, 2002.

[26] D. Kunii and O. Levenspiel, *Fluidization Engineering*, 2nd Edition, Butterworth-Heinemann, U.S.A, 1991.

[27] M. Z. Abdullah, Z. Husain, S.L. Yin Pong, "Analysis of cold flow fluidization test results for various biomass fuels," *Biomass and Bioenergy*, vol. 24, 2003, pp. 487 – 494.

[28] M. Wirsum, F. Fett, N. Iwanowa, G. Lukjanow, "Particle mixing in bubbling fluidized beds of binary particle systems," *Powd Tech*, vol. 120, 2001, p 63– 69.

[29] L.H. Shen, M.Y. Zhang, "Effect of particle size on solids mixing in bubbling fluidized bed," *Powd. Tech.*, vol. 97, 1998, pp. 170 – 177.

[30] P.C. Nicholas, P.C. Paul, *Hydrodynamics of Gas-Solids Fluidization*, Gulf Pub. Co. Houston, 1984.

[31] J.G. Yates, R.S. Ruiz-Martinez, D.J. Cheesman, "Prediction of bubble size in a fluidized bed containing horizontal tubes," *Chem. Eng. Sci.*, vol. 45, 1990, pp. 1105 – 1111.